Post-welding heat treating properties of 316L stainless steel and 600 nickel base alloy dissimilar weldment by GTAW

Chin-Pao Cheng*[1,2], Yang-Sheng You[1], Wei-Kang, Chiu[1]

[1]*Department of Mechatronic Engineering, National Taiwan Normal University, Taiwan*
[2]*Micro/Nano Device Inspection and Research Center, National Taiwan Normal University, Taiwan*

This study employed the inert gas tungsten arc welding technique to perform dissimilar joining of Inconel 600 nickel-based alloy and 316L stainless steel. The welding configuration adopted for the specimens was a butt joint. Additionally, the completed weldments underwent separate heat treatment processes: 24 hours of aging treatment at 700°C and 30 minutes of solution treatment at 1100°C. The experimental results revealed that after the inert gas tungsten arc welding, the hardness of welding zone, tensile strength, and elongation all exhibited a decrease, with the tensile fracture point located in the fusion zone of the weld. Following the 700°C aging treatment for 24 hours, there was an observable trend of improvement in the hardness of welding zone, tensile strength, and elongation. Upon undergoing the 1100°C solution treatment for 30 minutes, the elongation of weldments notably increased, while a decrease was observed in both yield strength and hardness.

Keywords: *Inconel 600 nickel-based alloy, 316L stainless steel, gas tungsten arc welding, post-welding heat treatment*

1. Introduction

Currently, the pressure vessels in nuclear power plants require the use of nickel-based alloys as materials in more demanding environments, while the outlet nozzles of the pressure vessels often employ materials like stainless steel or low-alloy steel to reduce costs [1-3]. In order to connect dissimilar metals from different parts, the gas tungsten arc welding (GTAW) technique is commonly used. However, due to the differences in microstructure, physical, and mechanical properties between the two distinct alloys, residual stresses can easily form at the interface after dissimilar welding, potentially leading to failures [4-6]. To ensure the quality of the reactor, it is essential to thoroughly investigate the welding properties and usage characteristics of stainless steel or low-alloy steel when combined with nickel-based superalloys [7].

Therefore, it is necessary to employ an appropriate welding method to join nickel-based alloys with stainless steel and to conduct suitable post-weld heat treatment to achieve optimal mechanical properties for specific applications [8-9]. This study aims to perform dissimilar joining through the GTAW process, with the introduction of inert gas to prevent material oxidation during welding. Due to the distinct properties of the two materials, proper welding parameters must be selected to achieve the desired welding quality. Various post-weld heat treatment conditions will be applied to compare their effects on mechanical properties. The welding process will involve thin plate butt joint welding without filler material to minimize the heat-affected zone and elemental redistribution effects caused by the welding zone.

2. Experimental method

The welding materials utilized in this study are Inconel 600 alloy and 316L stainless steel, both belonging to the austenitic series of alloys. The butt joint welding was performed using the gas tungsten arc welding (GTAW) technique without the addition of filler material, as shown in Figure 1. The experimental specimens had dimensions of 75mm × 50mm × 2mm for the thin plate. During the welding process, the backside of the weld was continuously back-purged with high-purity argon gas at a fixed flow rate. The welding current used was 80 amperes (A), and the welding travel speed was controlled at 100 mm/min. The welding voltage varied slightly due to manual operation. Finally, the completed welded specimens were placed in a heat treatment furnace for further processing. They underwent two distinct heat treatment processes: aging treatment (TT) at 700°C for 24 hours and solution annealing (SA) at 1100°C for 30 minutes. In this study, optical microscopy (OM) was utilized to observe the microstructures of the welded specimens before and after the heat treatment processes. Additionally, microhardness analysis and tensile tests were conducted to evaluate the mechanical properties of the weldments.

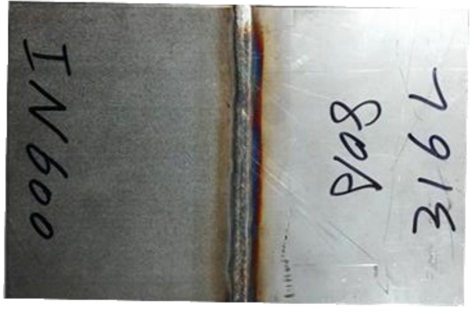

Figure 1 Appearance of the GTAW dissimilar specimen.

3. Results and discussion

3.1 Microstructure of dissimilar GTAW

After the GTAW of 316L stainless steel and Inconel 600 alloy, four distinct microstructural regions can be observed, as illustrated in Figure 2. These regions include the fusion zone, the interface zone, the heat-affected zone, and the base material zone. It is well-known that undercooling influences the solidification pattern of the molten metal. During the solidification of the remelted material in the fusion zone, the greater temperature gradient toward the

---

[*1] Professor, National Taiwan Normal University. Present address: 162, Section 1, Heping E. Rd., Taipei City 106, Taiwan.

[1] Master student, National Taiwan Normal University. Present address: 162, Section 1, Heping E. Rd., Taipei City 106, Taiwan.

material's edge leads to a smaller degree of undercooling. This results in the formation of a cellular dendritic structure, growing in the opposite direction to the maximum temperature gradient until a higher degree of undercooling generates columnar dendrites, thus giving rise to various solidification patterns in the fusion zone. The interface zone, positioned between the fusion zone and the heat-affected zone, showcases a distinct boundary line as the material falls around its melting point.

In the case of Inconel 600, epitaxial growth occurs along the grain boundaries. The direction of cellular dendrites aligns with the orientation of the original grains, while the interface zone extends toward the base material without exceeding its melting point, forming the heat-affected zone. Positioned between the interface zone and the base material zone, the heat-affected zone experiences grain growth due to the welding process surpassing the material's recrystallization temperature. This leads to the development of coarser grains without undergoing phase transformation during the process.

After subjecting the welded specimens to 700°C aging treatment for 24 hours, it is observed that the microstructure exhibits minimal changes compared to the pre-treatment state. The overall distribution of the four distinct regions remains present, but notable differences can be observed, as depicted in Figure 3. The growth direction of cellular dendrites remains aligned with the reverse direction of the maximum temperature gradient. Epitaxial growth is also evident for Inconel 600. Following the solution treatment at 1100°C for 30 minutes, the cross sectional microstructure of the weld, as illustrated in Figure 4, reveals extensive grain regrowth throughout the weld zone. Coarsening of grains is evident, making it less discernible to differentiate between the heat-affected zone and the base material zone.

Figure 2 Cross section microstructure of GTAW specimen: (left) SS 316L; (right) Inconel 600.

Figure 3 Microstructure of 700°C aging treatment specimen: (left) SS 316L; (right) Inconel 600.

Figure 4 Microstructure of 1100°C solution treatment specimen: (left) SS 316L; (right) Inconel 600.

3.2 Microhardness Analysis of Dissimilar GTAW

The microhardness distribution curve near the GTAW welding zone shown in Figure 5 indicates that the average hardness value of the base material is approximately 180 HV. In the central part of the fusion zone, the hardness is the lowest, reduced to around 140 HV. In the heat-affected zone, due to the coarsening of grains, the hardness is slightly lower than that of the base material. Clearly, when GTAW welding is performed without adding filler material, the fusion zone undergoes a new crystalline morphology, with a redistribution of grain structure and chemical composition. This could result in the loss of solid solution strengthening effect, leading to a decrease in hardness in this area.

After a 24-hour aging treatment at 700°C, the average hardness of the base material decreased to 170 HV. However, in the welding zone, the average hardness increased from the pre-heat-treated value of 140 HV to 160 HV, as shown in Figure 6. This increase might be attributed to the loss of solid solution strengthening characteristics in the initially re-melted weld zone. Nevertheless, following the aging treatment, the precipitation of carbides near grain boundaries has contributed to the enhancement of weld hardness. Furthermore, after a 30-minute solution treatment at 1100°C, the hardness distribution in the weld zone became more uniform without distinct boundaries. The overall hardness decreased from 180 HV in the base material to 135 HV. This can be attributed to the dissolution of carbides and strengthening phases due to the solution treatment, coupled with the occurrence of grain growth. As a result, the hardness has significantly decreased.

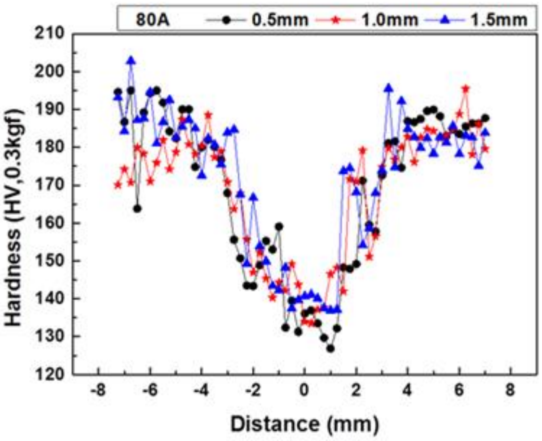

Figure 5. Microhardness distribution curve of welding zone in the as welded specimen.

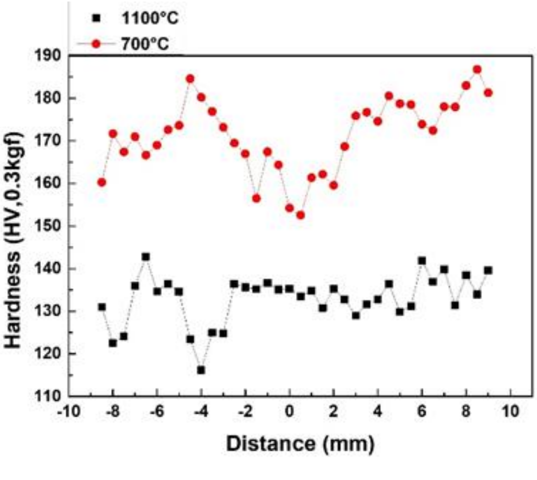

Figure 6. Microhardness distribution curve of welding zone in the Post-welding heat treating specimen.

3.3 Tensile properties of dissimilar GTAW

Table 1 presents the tensile properties of the base material and GTAW-80A specimens after different treatments, with the tensile fractures all occurring within the fusion zone. Following a 24-hour aging treatment at 700°C, there is a slight decrease in yield strength, but both ultimate tensile strength and elongation show improvement. Yield strength decreases from 319.4 MPa prior to heat treatment to 290.7 MPa, while ultimate tensile strength increases from 475.6 MPa to 535.5 MPa, and elongation rises from 15.2% to 24.2%. The phenomenon of chromium carbide precipitation commonly occurs in welds subjected to a 700°C, 24-hour aging treatment, reinforcing grain boundaries and enhancing overall mechanical properties. After a 30-minute solution treatment at 1100°C, a marginal increase in ultimate tensile strength is observed, coupled with a significant improvement in elongation. However, there is a notable decrease in yield strength. Yield strength drops to 164 MPa, while ultimate tensile strength rises to 519.2 MPa, and elongation increases to 55%.

Table1. Tensile properties of the test specimens.

	YS (MPa)	**TS (MPa)**	**E (%)**
SS 316L	342.9	642.9	66.3
Inconel 600	357.0	654.3	48.2
As welded	319.4	475.6	15.2
1100°C	164.0	519.2	55.1
700°C	290.7	535.5	24.2

4. Conclusion

1. Utilizing the inert gas tungsten arc welding (GTAW) method, successful joining of Inconel 600 alloy and 316L stainless steel is achieved with a welding current parameter of 80A, resulting in defect-free welds. Near the weld zone, distinct regions can be observed including the fusion zone, transition zone, heat-affected zone, and base material. The fusion zone exhibits a cellular, dendritic, and equiaxed grain structure. On the other hand, the heat-affected zone experiences coarsening of grain size.
2. Prior to heat treatment, there is a decrease in hardness within the welding zone. However, after a 24-hour aging treatment at 700°C, the average hardness of the weld zone increases from the pre-heat-treated value of 140 HV to 160 HV. Furthermore, following a 30-minute solution treatment at 1100°C, the hardness distribution in the weld zone becomes more uniform, resulting in an overall decrease in hardness from 180 HV in the base material to 135 HV.
3. After a 24-hour aging treatment at 700°C, there is a slight decrease in the yield strength of the weld zone. However, both the ultimate tensile strength and elongation show improvement. Following a 30-minute solution treatment at 1100°C, there is a marginal increase in ultimate tensile strength, and the elongation rises to 55%. Nevertheless, the yield strength experiences a decrease.

Acknowledgment

This work was sponsored by the Minister of Science and Technology under Contracts MOST 105-2221-E-003-005.

References

1. S. Hwang: Journal of Nuclear Materials **443** (2013) 321-330.
2. X. Zhong, S.C. Bali, T. Shoji: Corrosion Science **118** (2017) 143-157.
3. T. Poulain, J. Mendez, G. Henaff, L.D. Baglion: Procedia Engineering **160** (2016) 123-130.
4. A. Joseph, S.K. Rai, T. Jayakumar , N. Murugan: International Journal of Pressure Vessels and Piping **82** (2005) 700-705.
5. C.H. Lee, K.H. Chang: Applied Thermal Engineering **45-46** (2012) 33-41.
6. R. Mouginot and H. Hännine: Aalto University, Finland, (2013).
7. N. Kumar, C. Pandey, P. Kumar: Journal of Pressure Vessel Technology **145** (2023) 011506-1~011506-25.
8. C.A. Huang, T.H. Wang, C.H. Lee, W.C. Han: Materials Science and Engineering A **398** (2005) 275-281.
9. A. Sukumaran, R.K. Gupta, and V. A. Kumar: Journal of Materials Engineering and Performance **26** (2017) 3048-3057.